International Journal of Heat and Mass Transfer 179 (2021) 121642

Contents lists available at ScienceDirect

International Journal of Heat and Mass Transfer

journal homepage: www.elsevier.com/locate/hmt

Experimental investigation on wettability and capillary performance of ultrasonic modified grooved aluminum wicks

Guisheng Zhong[a,b], Yong Tang[a], Xinrui Ding[a,*], Gong Chen[a], Zongtao Li[a]

[a] School of Mechanical and Automotive Engineering, South China University of Technology, Guangzhou 510640, China
[b] Department of Mechanical Engineering, University of South Carolina, Columbia 29208, USA

ARTICLE INFO

Article history:
Received 8 April 2021
Revised 5 June 2021
Accepted 24 June 2021

Keywords:
Ultra-thin flat heat pipe
Aluminum groove
Ultrasonic modification
Porous microstructures
Capillary performance

ABSTRACT

The grooved wick has a promising potential in the field of ultra-thin flat heat pipes, and the porous structure can improve the capillary performance of grooved wicks significantly. In this paper, an environmentally friendly method, named as ultrasonic modification, was developed to fabricate porous microstructures on grooved aluminum wick. The effects of ultrasonic modification times on the morphology, wettability and capillary performance of the porous grooved wick were investigated. The results indicate that appropriate ultrasonic modification times can realize an excellent distribution of porous microstructures throughout the groove surface. After ultrasonic modification, the modified surface became hydrophobic since the porous microstructures were covered with a low-surface-energy coating. However, in case of aluminum heat pipes with acetone as working liquid, the wettability and capillary performance of the modified grooved wick can still be enhanced significantly. The maximum capillary rise height and the capillary performance parameter of the modified grooved wicks were increased for a factor of 3 and an order of magnitude, respectively. This study provides a new idea for the fabrication of porous aluminum wicks, which is beneficial to promote the development of ultra-flat aluminum heat pipes.

1. Introduction

With the miniaturization of high-performance electronics, thermal management of these microelectronic systems has become a new challenge for the current heat pipe technology. Due to the limited space for heat dissipation and higher heat flux in the microelectronic systems, the acceptable heat pipes must possess small dimensions with excellent heat transfer capacity. Ultra-thin flat heat pipes have attracted the attention of the microelectronic industry for thermal management application, due to their advantages such as high thermal conductivity, thinner thickness and facility to accommodate multiple heat components [1,2].

The most significant component in ultra-thin flat heat pipes is the wick which affect the thermal performance of heat pipe directly owing to its capillary performance. The common wicks used in the flat heat pipes include groove [3,4], sintered powder [5,6], mesh [7,8], and micropillar [9]. Among them, the sintered powder and mesh normally generate better capillary performance than the groove, so the flat heat pipes with sintered powder or mesh wicks usually reach higher heat transfer capacity than those with grooved wicks. However, the increasing capillary pressure of wicks will reduce the permeability and vice versa [10]. The lower permeability can limit the thermal performance of flat heat pipes reversely. Besides, compared with the sintered powder and mesh wick, the grooved wick with higher permeability can be fabricated on the internal surface of flat heat pipes more simply and directly, which is more stable and yields more space for vapor flow. Hence, considering the heat transfer stability and the limited space of ultra-thin flat heat pipes, the grooved wick shows more promising potential in the fabrication of ultra-thin flat heat pipes.

Many scholars have focused their studies on the capillary performance enhancement of grooved wicks to improve the maximum heat transport capability of flat heat pipes [11–18]. As a traditional and effective method, composite grooved wicks have been reported widely in copper flat heat pipes. Deng et al. [11] fabricated a composite wick by covering a layer of sintered copper powder on the micro *V*-grooves. The composite wick enhanced the capillary pressure for about 2–4 times compared to the grooved wick. Wong and Liao [12] studied the thermal performance of flat-plate heat pipes with composite mesh-groove wick. The maximum heat load was increased by 3 times due to the combinative advantages of high capillarity from the mesh screen and high permeability of the parallel grooves. Zeng et al. [14] proposed a novel micro-grooved wick with reentrant cavity array. The experimental results indicated that the novel wick could enhance the capillary rise with

* Corresponding author.
E-mail address: dingxr@scut.edu.cn (X. Ding).

https://doi.org/10.1016/j.ijheatmasstransfer.2021.121642
0017-9310/

Nomenclature

ΔP_c	capillary pressure, [Pa]
ΔP	pressure drop, [Pa]
K	permeability, [m^2]
R_{eff}	effective pore radius, [m]
$\Delta P_c \cdot K$	capillary performance parameter, [N]
g	gravitational acceleration, [m/s^2]
h	capillary height, [m]
dh/dt	capillary rise velocity, [m/s]
t	time, [s]
k	slope of the fitting line, [m^2/s]
r_c	the capillary radius, [m]

Greek symbols

σ	surface tension, [N/m]
ρ	density of liquid, [kg/m^3]
μ	dynamic viscosity of liquid, [Pa·s]
θ	the contact angle, [°]

Subscript

f	friction
g	gravity
eff	effective

little penalty of pressure drop. They also developed an aluminum vapor chamber using the micro-grooved wick with reentrant cavity array and the excellent thermal performances under various operational conditions were further verified [15]. The surface morphology of grooves also plays an important role in the capillary performance of grooved wicks. Huang et al. [16] proposed a chemical corrosion method to change the surface morphology of the grooved wick for capillary performance enhancement. The study revealed that the optimal corrosion parameter could gain a capillary performance enhancement of 155%. Tang et al. [17] studied the effect of chemical corrosion on the capillary performance of micro *V*-grooves wick fabricated by ploughing–extrusion. Only a maximum increase of 96.33% in capillary rise height was achieved. Lu et al. [18] developed a composite wick with a porous layer on the rectangular copper grooves by electrochemical deposition. The capillary performance parameter of the composite wick was enhanced by more than 20% with the optimal deposition parameters. The common feature of the above methods is to construct porous microstructures on the groove surface. However, both chemical corrosion and electrochemical deposition processes may produce polluting effluents and increase economic costs. It seems that an environment-friendly and effective method to improve the capillary performance of grooved wicks is still urgently required. Further comparing the enhancement mechanism of the above methods, the composite grooved wicks with micro/nanostructures exhibit better capillary performance, which can further improve the maximum heat transport capability of the heat pipe. Besides, ultrasonic has been widely used in the industry, involving cleaning, machining, and pharmaceutical manufacture. Ultrasonic cavitation is the most important characteristic during ultrasonic treatment. Virot et al. [19] evidenced that ultrasonic cavitation can increase the roughness and wettability of Si wafer. Skorb et al. [20] reported that ultrasonic cavitation can induce oxidation of metal surface and etching of metal matrix to form mesoporous metal sponges. Therefore, it is possible to employ ultrasonic cavitation to enhance the groove wick in the heat pipe industry. And related research has not been reported yet.

In this paper, an environmentally friendly method, named as ultrasonic modification, was developed to fabricate porous grooved aluminum wicks for ultra-thin flat heat pipes. It is also a novel method for solving the manufacturing problem of porous aluminum wick due to the hindrance effect of aluminum oxide film on sintering [21]. During ultrasonic modification, cavitation bubbles caused by ultrasonic vibration underwent the procedures of generation, growth, pulsation and collapse [22,23]. Under the impact of the microjets caused by cavitation bubble collapse, porous microstructures were created directly on the groove surface, which is different from the sintering process. The forming process of porous microstructures was controlled by changing the ultrasonic modification times. The morphology, wettability and capillary performance of the modified grooved wicks were investigated comprehensively. Moreover, the capillary performance of the porous grooved aluminum wicks was assessed with the capillary rise height and capillary performance parameter.

2. Experiment

2.1. Sample preparation

The grooved wick used in this study was fabricated by aluminum extrusion with the dimension of 160 mm × 80 mm (see Fig. 1a), and the samples were cut into approximately 100 mm × 10 mm by wire cutting (see Fig. 1b). As shown in Fig. 2, the ultrasonic modification process was performed on a custom-built apparatus. The ultrasonic generator (SXSONIC FS-300 N) operating at a vibration frequency of 20 kHz was mounted at a computer-controlled *X*-*Z*-direction holder. Ultrasonic vibration was created by the generator in the vertical direction and amplified by the horn to generate ultrasound waves at the end of the horn tip. The diameter of the horn tip used in this study is 8 mm and the ultrasonic amplitude is 75 μm. The workpiece was mounted at the bottom of an opening container fixed at a *Y*-direction working stage. The minimum step size in all three directions is 5 μm. Tap water was selected as the liquid medium in which cavitation bubbles can grow and collapse to form impact force to process the groove surface. And the volume of water required should be enough to completely submerge the horn tip during the modification process. To ensure the consistency of all modification experiments, the distance between the water surface and the end of the horn tip was always maintained at about 10 mm.

Prior to the modification, the horn tip was moved to touch the top of the grooves at five different positions along the direction of the groove and the positions of the groove sample relative to the horn were calculated and recorded in the computer. The modification process was accomplished by a computer program that moved the vibrating horn toward one end of the workpiece to a constant clearance of 0.5 mm, then moved along the groove to the other end of the workpiece at a speed of 0.4 mm/s and returned (see Fig. 2b). In the modification process, cavitation bubbles nucleate and grow in the liquid where the local pressure is lower than the saturated vapor under the action of ultrasound waves. As the bubbles approach the solid surface, the pressure distribution on the bubble surface becomes asymmetric, so they will collapse and produce microjets towards the solid surface. The intense impact of the microjets may further change the surface morphology of the grooves [23,24]. In order to study the effect of modification duration, the above modification process was repeated 3 times (S2), 5 times (S3) and 7 times (S4), respectively. The results were compared with the untreated one (S1). In addition, a water bath and a peristaltic pump were utilized to circulate the water in the container and maintained the water temperature of 25 °C during the modification process. After ultrasonic modification, the samples were subjected to ultrasonic cleaning in ethanol for 3 min to remove residual moisture and impurities, and then the samples were dried by nitrogen flow.

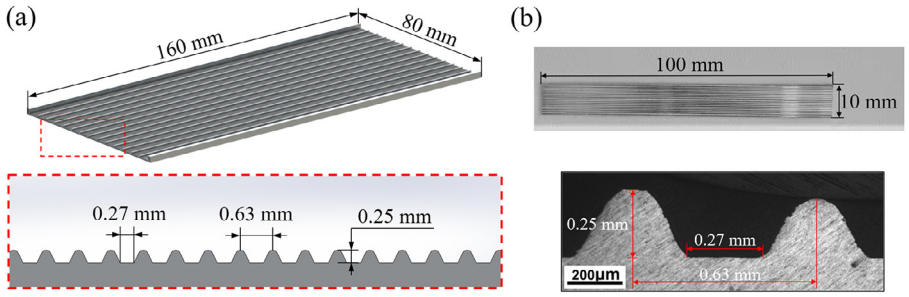

Fig. 1. (a) Schematic of the grooved aluminum wick, (b) image of the grooved wick sample.

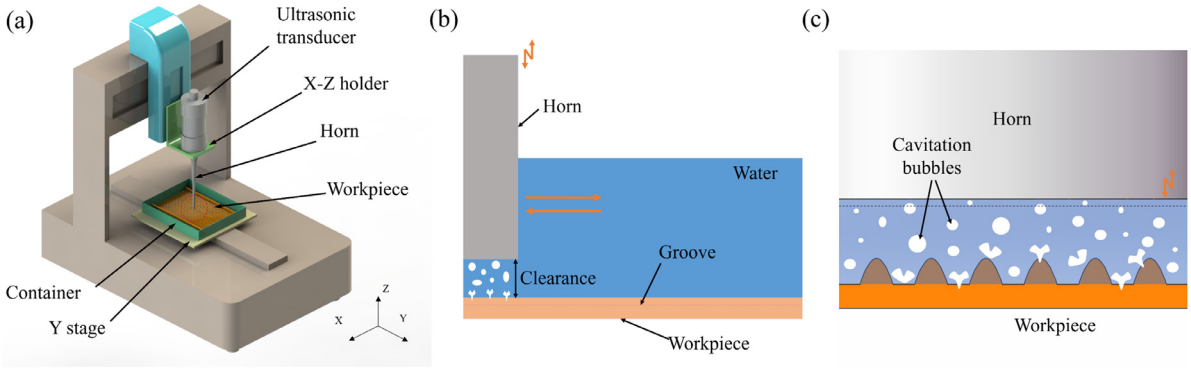

Fig. 2. Schematics of the (a) ultrasonic modification apparatus, (b) ultrasonic modification process, and (c) ultrasonic cavitation.

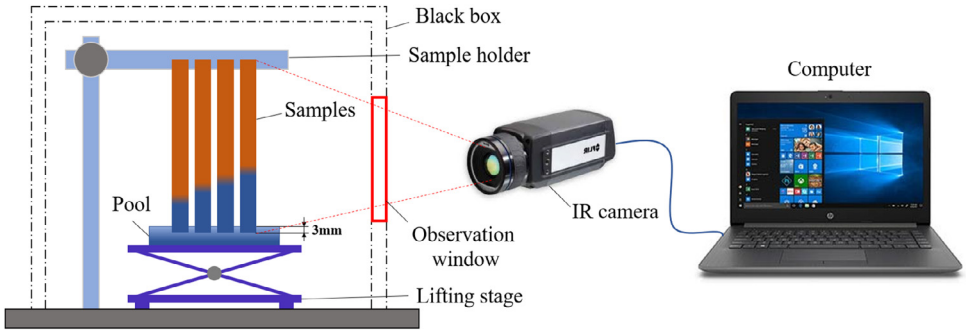

Fig. 3. Schematic of the capillary rise test setup.

2.2. Capillary rise test

The capillary rise of the modified grooved wicks was measured using an IR thermal imaging method which has been widely applied in many research works on capillary performance [12,14,17,25,26]. The schematic of the test setup is shown in Fig. 3. An IR thermal imaging camera (FLIR A615, FOV 15°) with the thermal sensitivity of 0.05 K was utilized to capture the capillary rise process of liquid in the aluminum grooves at a frame frequency of 25 Hz. The resolution of the IR thermal images is 640 × 480 pixel. Comparing the pixel point with the length of the samples, one pixel corresponds to 0.26 mm with the validation. Apart from the IR thermal imaging camera, the test setup consisted of a lifting stage, a sample holder, a liquid pool, a computer and a black box with an observation window. Before the test, the samples were mounted on the sample holder with the bottom ends of all samples at the same height. During the measurement, the samples were immersed into the working liquid by moving upward the lifting stage and the immersion depth was controlled at 3 mm. Subsequently, the liquid rose along the groove sample due to the capillary pressure generated by the groove and its surface microstructures. The dynamic process of the meniscus movement in the grooves was recorded by the IR-camera due to the difference in emissivity between metal and liquid. The test lasted 90 s and then the capillary heights in the IR thermal images were extracted and visualized on the computer. To reduce the effect of the surrounding environment, the black box was used to minimize the liquid evaporation and prevent the light influence. The ambient temperature was maintained at 25 °C.

2.3. Data analysis for capillary performance parameter

In general, the capillary performance parameters ($\Delta P_c \cdot K$) and (K/R_{eff}) are usually used to evaluate the capillary performance of wicks in various related researches [12,14,16–18]. For the capillary performance parameter (K/R_{eff}), it is difficult to determine the effective pore radius R_{eff} of the grooves with irregular microstructures. Therefore, the capillary performance parameter ($\Delta P_c \cdot K$) integrating capillary pressure ΔP_c and permeability K is employed for a comprehensive evaluation of the modified grooved wicks in the present study. According to the momentum balance, the head pressure balance of the groove in the liquid can be given [17,27]:

$$\Delta P_c = \Delta P_f + \Delta P_g = \frac{2\sigma}{r_c}\cos\theta \tag{1}$$

Where ΔP_f is the viscous friction pressure drop, ΔP_g is the hydrostatic pressure drop due to gravity, σ is the surface tension of the liquid, r_c is the capillary radius, and θ is the contact angle. Therefore, Eq. (1) can be rewritten as [14]:

$$\Delta P_c = \frac{\mu h}{K}\frac{dh}{dt} + \rho g h \tag{2}$$

Where μ is the viscosity of liquid, h is the capillary height, dh/dt is the capillary rise velocity, ρ is the density of liquid and g is the gravitational acceleration.

As proposed in the literature [14,28], the capillary rise can be regarded as viscous dominated flow in the initial stage by neglecting the gravitational effect. With this assumption, Eq. (2) can be rearranged and solved with the initial condition h $(t \to 0) = 0$, and the result is [28]:

$$h^2 = \frac{2\Delta P_c \cdot \mathrm{K}}{\mu} t = k_1 t \tag{3}$$

Therefore,

$$\Delta P_c \cdot \mathrm{K} = \frac{\mu k_1}{2} \tag{4}$$

From Eq. (3), it is seen that h^2 and t are fitted in a linear correlation in the case of viscous dominated flow. Hence, $\Delta P_c \cdot K$ in the initial stage can be calculated by the slope k_1 of the fitting line of Eq. (3). However, as the capillary height continues to increase, the effect of gravity cannot be neglected anymore and the Eq. (4) is not suitable for the prediction of $\Delta P_c \cdot K$.

Considering the effect of gravity, rearranging Eq. (2) yields [16,18]:

$$\frac{dh}{dt} = k_2 \frac{1}{h} - \frac{\rho g K}{\mu} \tag{5}$$

$$k_2 = \frac{\Delta P_c \cdot K}{\mu} \tag{6}$$

It is obvious that a linear fitting can also be obtained between dh/dt and $1/h$. Then, $\Delta P_c \cdot K$ can be calculated using the slope k_2 of this fitted line.

2.4. Uncertainty analysis

The uncertainty in the experiment is estimated based on the random errors in the capillary rise measurements. The relative measurement errors of capillary rise height, capillary rise velocity, and capillary performance parameter are calculated using the uncertainty analysis method [29]:

$$\frac{e(f)}{f} = \frac{\sqrt{\sum \left(\frac{\partial f}{\partial x_i} e_{x_i}\right)^2}}{f} \tag{7}$$

where $e(f)$ is the measurement error of the variable f, and e_{xi} is the maximum measurement error of each section defined as x_i. The uncertainties of capillary rise height and capillary rise velocity are estimated to be within 4.72% and 6.18%, respectively. With the standard deviation of the capillary performance parameter by linear fitting, the uncertainty of $\Delta P_c \cdot K$ is estimated to be within 8.04% in the initial stage while at the zone with gravity influence it is within 8.47%.

3. Results and discussion

3.1. Morphology of the modified grooves

Fig. 4 shows the 3D image of the aluminum groove structure. Comparing with the bare grooved wick, the dimension of the modified groove structure was only slightly changed. The groove surfaces seemed to become rougher after ultrasonic modification, especially the bottom of the grooves. For comprehensive and detailed characterization, the samples were observed under a scanning electron microscope (SEM) at three magnifications of 100 × , 400 × and 5000 × . The SEM images of the sample surfaces are presented in Fig. 5. It is obvious that ultrasonic modification has a great effect on the morphology of the aluminum grooves. As depicted in Fig. 5a, the original wick only consisted of several small and shallow grooves with relatively smooth surface. As the ultrasonic modification proceeded, the bare groove surface became rougher with the appearance of a layer of porous microstructures. Under the 100 × magnification, it is found that the porous microstructures were fabricated at the bottom of the grooves, followed by expanding to the top of the grooves as modification times increased. It means that the first area impacted by cavitation bubble collapse is the bottom of the grooves and then the top followed. As common sense, the formation of a bubble requires a nucleation site. Compared with other areas of the grooves, the bottom corners of the grooves have a relatively small curvature ra-

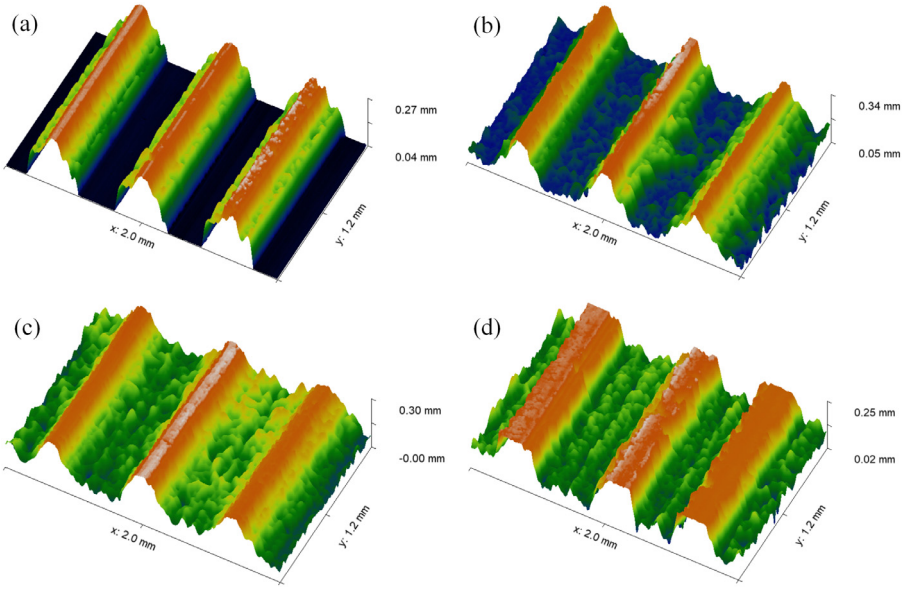

Fig. 4. 3D image of the aluminum groove structure: (a) S1, (b) S2, (c) S3, and (d) S4.

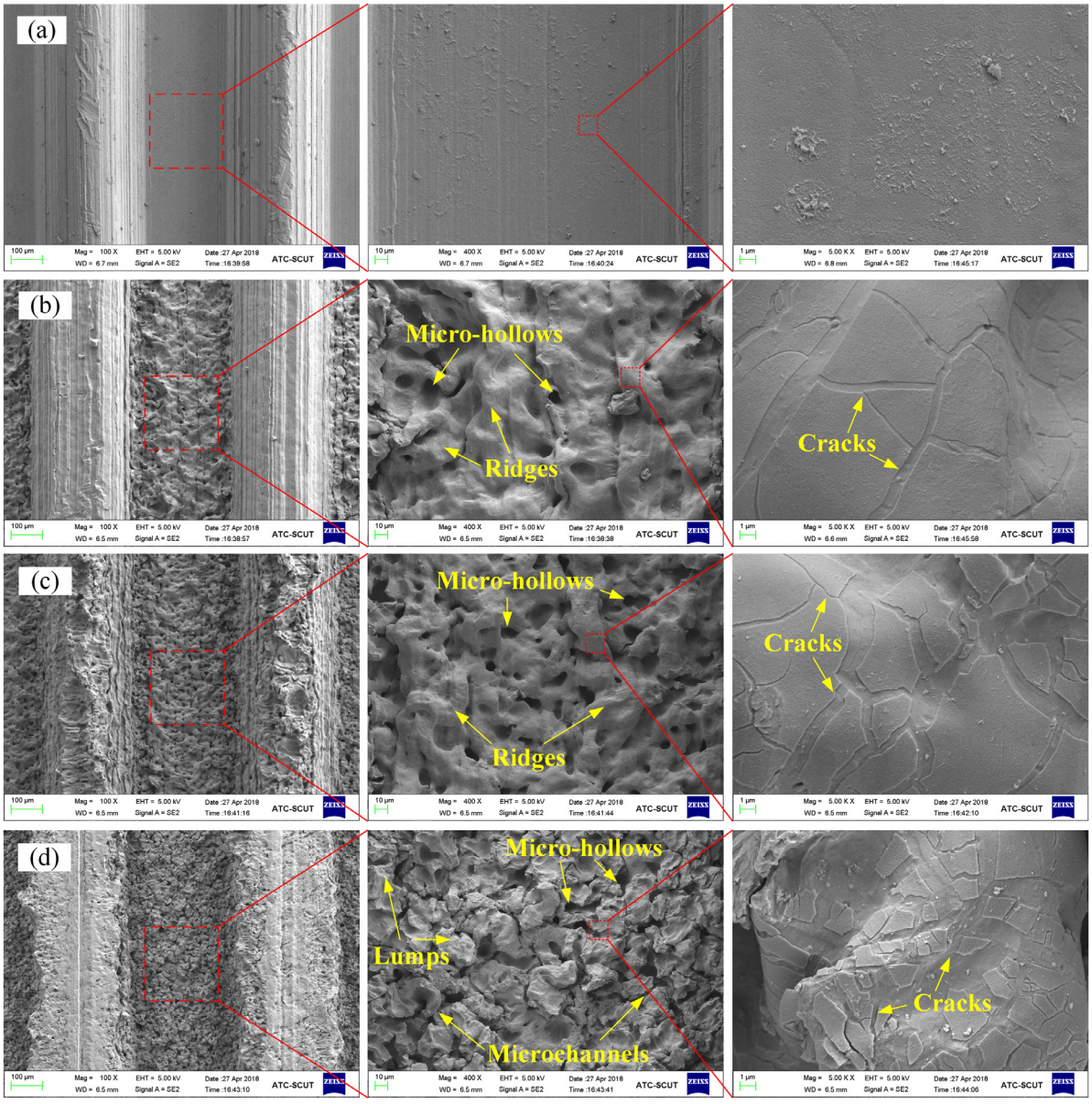

Fig. 5. SEM images of the aluminum grooves: (a) S1, (b) S2, (c) S3, and (d) S4.

dius, which can work as potential nucleation sites. During ultrasonic cavitation, these nucleation sites are beneficial for the formation of cavitation bubbles and promote their evolution. Hence, the bottom area may suffer intense impact caused by cavitation bubble collapse preferentially, leading to the appearance of porous microstructures. Moreover, when the modification times were increased to 7, the top of the groove was damaged, and a rough plane was formed because of the long-time cavitation collapse impact. It is indicated that controlling the modification times can achieve the fabrication of the porous microstructure only at the bottom of the grooves. For the aluminum grooved wick used in the study, it can be realized by repeating the modification process 3 times. Under the 400 $\times$ magnification, the bottom of the grooves was changed to a coarse rock-shaped morphology with numerous dead-end micro-hollows and ridges under the impact of ultrasonic cavitation bubbles. The dimensions of the micro-hollows were measured using ImageJ software at multiple locations. The average diameters of the micro-hollows were 17.9 μm, 15.4 μm and 12.9 μm for S2, S3 and S4, respectively. Obviously, the diameter of the micro-hollows decreased slightly with the increasing modification times. Meanwhile, as increasing the modification times, the density of micro-hollows further increased, the ridges were further disintegrated into coarser and smaller lumps, and then the interconnect microchannels were formed between the micro-hollows. Both micro-hollows and interconnect microchannels constituted the porous microstructures on the groove surface. Under the 5000 $\times$ magnification, the complexity of the rock-shaped morphology can be further indicated by the number of micro-scale cracks on the surface which increased with the modification times. It is indicated that the longer the modification time is, the more severe deformation the groove surface suffers. Namely, as the modification time per unit area increases, both the cavitation impact per unit area and the extent of modification are enhanced, thereby leading to a more abundant rock-shaped morphology on the groove surface. On the other hand, it also causes damage to the top of the grooves to some extent if the cavitation impact time is excessive.

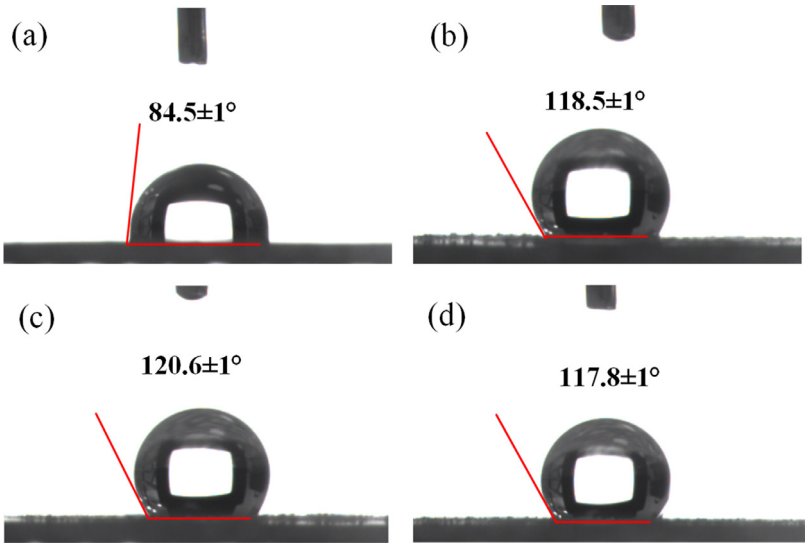

Fig. 6. Contact angle images of water on the plane surface: (a) S1, (b) S2, (c) S3 and (d) S4.

3.2. Wettability test

The similar modification processes were performed on plane surfaces for exploring the wettability of the modified surfaces. For better understanding the wetting properties of the modified surfaces with different surface tension liquids, both water (surface tension of 72.1 mN/m) and acetone (surface tension of 23.3 mN/m) were used as the indicator and the droplet volume for each characterization was 4 μl. The surface contact angle was measured by a contact angle measurement system (Powereach, JC2000D, China) with an accuracy of ± 1° Fig. 6 depicts the shape of water droplets on the aluminum surfaces modified with different modification times. As shown in Fig. 6, the original contact angle of water on the smooth surface was 84.5 ± 1°, while the contact angles on all modified surfaces were about 120° It is obvious that the aluminum surfaces were transformed from slightly hydrophilic to moderately hydrophobic after ultrasonic modification. Comparing with the smooth surface, the modified surface had a larger surface roughness ratio due to the appearance of porous microstructures. According to the Wenzel model [30], the modified surface should have become more hydrophilic. However, during ultrasonic modification the collapsing cavitation bubbles can create transient local areas of high temperature more than 5,000 K and high pressure of about 1,000 atmospheres [31]. Since the initial protective layer of oxide have been destroyed during ultrasonic modification, the unprotected surface will be further rapidly modified by highly reactive radicals and oxygen from water. Hence, the surface chemistry of the porous microstructures should be different, which may change the surface energy and then wettability of the whole aluminum surface. The surface chemistry of the porous microstructures was analyzed by energy-dispersive X-ray spectroscopy (EDS, Oxford X-MAX, UK) and Fourier transform infrared spectroscopy (FT-IR, Nicolet IS50-Nicolet Continuum, USA). After ultrasonic modification treatment, the modified aluminum surface showed a clear increase in carbon content and a slight decrease in oxygen content, as shown in Table 1. It can be explained that under the influence of extreme temperature and pressure the unprotected aluminum surface can easily react with oxygen and water, resulting in the formation of AlOOH and Al_2O_3 on the porous microstructures [32]. In the previous literature [33–35], organic adsorption was observed on aluminum oxide and metal oxides with an–OH group. Therefore, AlOOH and Al_2O_3 could adsorb organic matter from the ambient water and this process was accelerated under high temperature

Table 1
Chemical composition of the original aluminum surface (S1) and the modified aluminum surface (S2–S4) with different modification times.

Element	S1	S2	S3	S4
C	14.99	24.77	29.71	22.68
O	5.45	2.20	2.54	2.16
Al	78.47	71.70	66.15	73.96
Mn	1.09	1.33	1.60	1.20
O/Al	0.07	0.03	0.04	0.03
C/Al	0.19	0.35	0.45	0.31

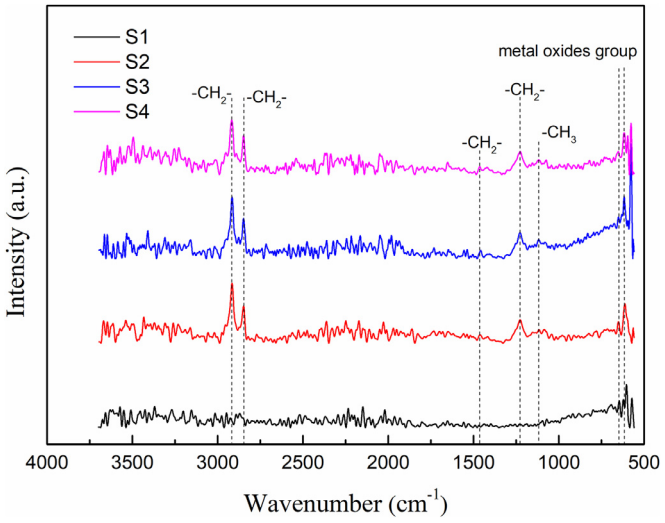

Fig. 7. FT-IR results of original aluminum (S1) and ultrasonic-modified aluminum (S2–S4).

condition, causing the appearance of hydrophobic groups (–CH_3,–CH_2–) [36], which is demonstrated in Fig. 7. These hydrophobic groups helped to form a low-surface-energy coating on the porous microstructures so that the modified surface became hydrophobic. Namely, the combined effect of rough porous aluminum surface coupled with organic matter leads to the opposite change in wettability of the modified surface with water, which be explained by the Cassie–Baxter model [37].

Obviously, the hydrophobic aluminum surface is not beneficial to the improvement of the capillary performance of the aluminum

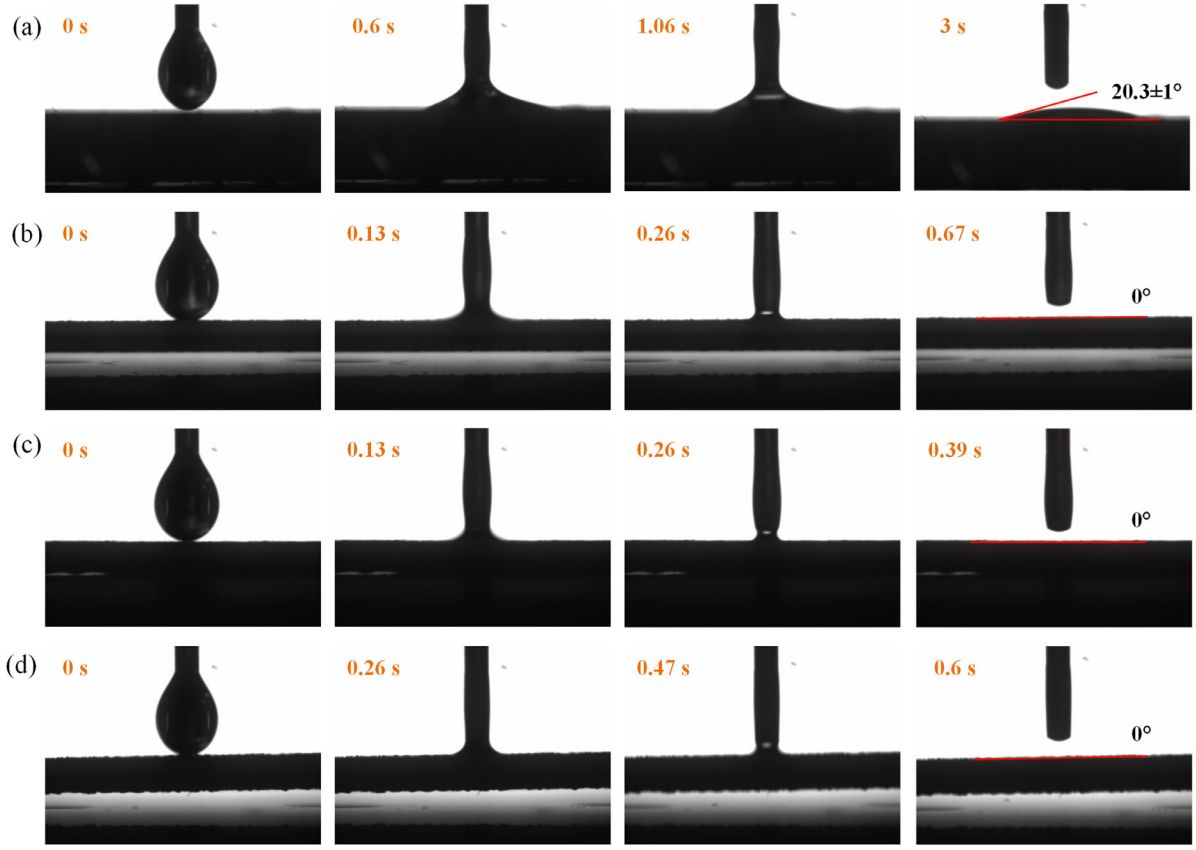

Fig. 8. Contact angle images of acetone on the plane surface: (a) S1, (b) S2, (c) S3 and (d) S4.

grooved wicks. However, due to the incompatibility between aluminum and water, water cannot be used as the working liquid in the aluminum heat pipes. On the other hand, many low surface tension liquids have been widely used as the working liquid in the manufacture of aluminum heat pipes, such as acetone and HFC-7100, whose wetting performance on the aluminum surface is different from water due to their difference in surface tension. Hence, in order to explore the effect of porous microstructures with a low-surface-energy coating on the wetting performance of the working liquid in aluminum heat pipes, it is necessary to conduct a similar contact angle test with acetone.

In our preliminary experiment, acetone spread fast on the modified aluminum surface. The complete spreading processes of acetone on the modified plane surfaces were recorded and shown in Fig. 8. The apparent contact angle of acetone on the bare aluminum surface was 20.3 ± 1°, indicating that the original aluminum surface was oleophilic. For the modified surfaces, acetone was absorbed into the modified surface within 1 s upon it touched the surface. As shown in Fig. 8, the static contact angles of acetone on the modified surfaces were nearly 0°, indicating that the hydrophobic modified aluminum surface was readily wetted by acetone. It is demonstrated that the low-surface-energy organic matter coating on the modified aluminum surface has no negative effect on the wetting of acetone, while the porous microstructures can promote the complete wetting of acetone on the modified surface. It can be concluded that the aluminum surface became hydrophobic and superoleophilic after ultrasonic modification treatment.

3.3. Capillary rise test

Capillary rise height is an important index for the capillary performance evaluation of the wick in heat pipes. Based on the above analysis and the wettability test results of the modified aluminum surface, acetone was chosen for the subsequent capillary performance evaluation. Fig. 9 shows a series of IR images of the four wick samples at six specific time. It is obvious that the liquid in all wick samples rose rapidly within 15 s, and then the capillary rise velocity tended to be gentle after 15 s until the quasi-static equilibrium state occurred. For a more intuitive analysis, the capillary rise heights at different time were measured and connected via *B*-Spline as shown in Fig. 10. The capillary rise height in the first 5 s was almost proportional to time, which is regarded as the initial stage. And the following capillary rise stage is noted as the long-time stage in which the liquid rose at a decreasing rate due to the effect of gravity. By comparing the capillary rise height of the four wicks, it is apparent that the modified wicks exhibited faster rise velocity and higher rise height than the bare grooved wick while the difference between these modified wicks was very slight. It seems that the micro-hollows on the groove surface can remarkably reduce the capillary radius of the grooved wick. According to Eq. (1), these micro-hollows will provide extra capillary force to promote the flow of liquid in the interconnect microchannels against gravity. It is indicated that the low-surface-energy coating on the modified surface has a negligible effect on the capillary performance of grooved wick with acetone as the working liquid, which is in accord with the result of wettability test. On the other hand, according to the observation in Fig. 5, the slight difference between these modified wicks indicates that the porous microstructures at the bottom of the groove can enhance capillary performance more significantly than that at the sidewall of the groove. Namely, excessive modification cannot further significantly enhance the capillary performance of the groove wicks, if the depth of the ultrasonic modification can reach the bottom of the groove to fabricate porous microstructures sufficiently. The color of the liquid in the modified grooves became darker after

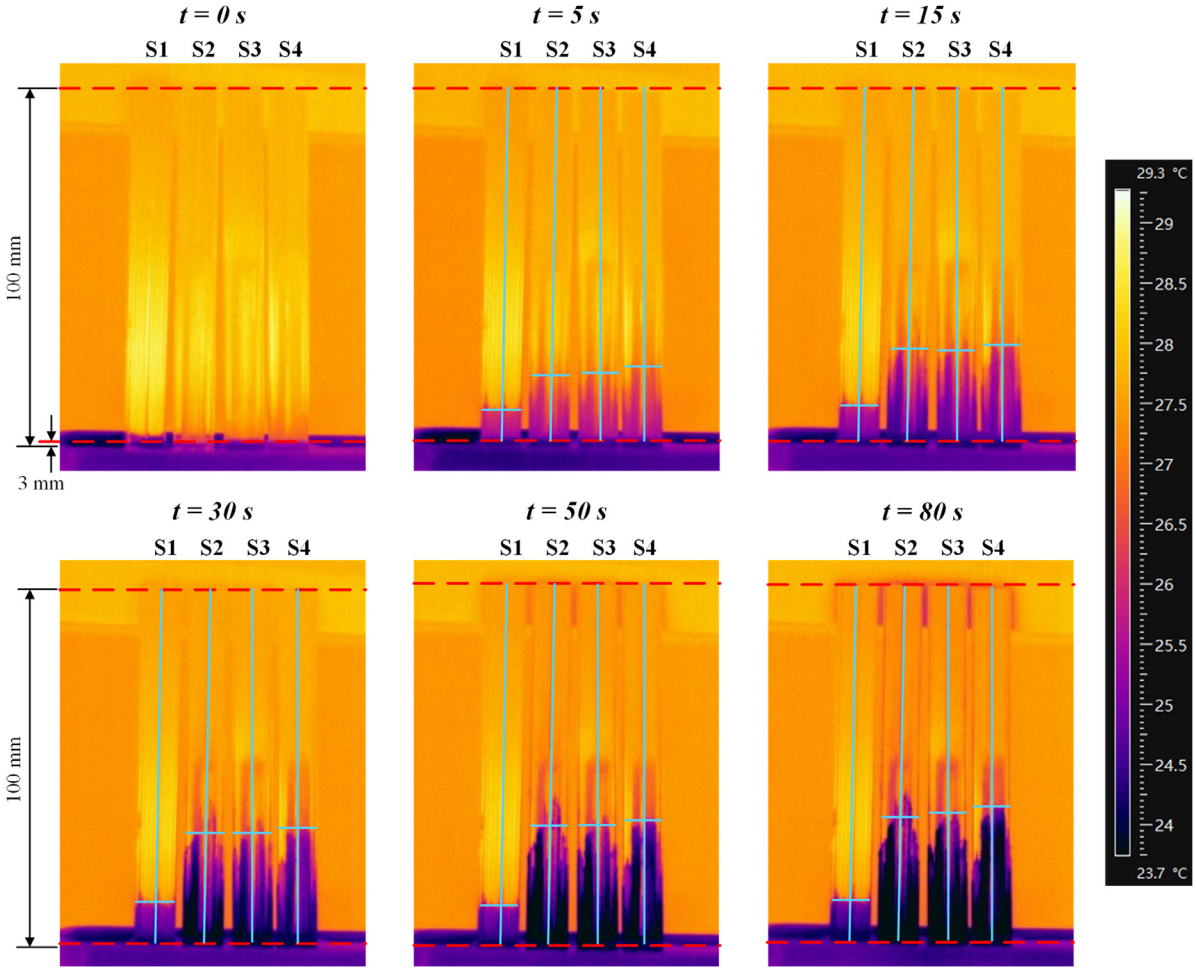

Fig. 9. IR images of capillary rise processes of the grooved wicks at six specific time.

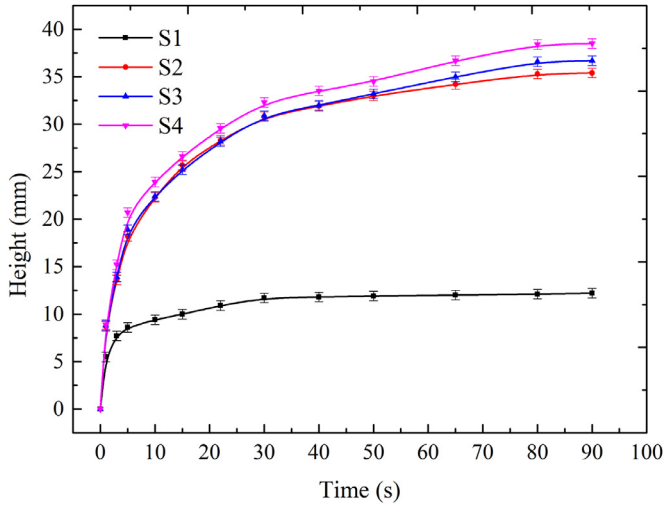

Fig. 10. Measured capillary rise height as a function of time for the grooves with different modification times.

30 s in Fig. 9, indicating that more working liquid was adsorbed in the modified grooves due to the porous microstructures. The adsorption of the working liquid supported the second capillary rise at a low velocity, corresponding to the rising process between 30 and 80 s in Fig. 10. The similar phenomenon was also reported by Zeng et al. [14]. As depicted in Fig. 10, the capillary rise heights

Table 2
The calculation results of capillary performance parameter ($\Delta P_c \cdot K$).

Sample	$\Delta P_c \cdot K$ (N)	
	Without gravity Eq. (3)	With gravity Eq. (5)
S1	7.35e−6	3.22e−6
S2	3.52e−5	3.38e−5
S3	3.81e−5	3.21e−5
S4	4.63e−5	3.42e−5

of the modified wicks were about 35.1 mm, while that of the bare grooved wick was only about 11.4 mm, indicating an increase for approximately a factor of 3 in the maximum capillary rise height.

In order to calculate the capillary performance parameter ($\Delta P_c \cdot K$), the linear fits between the square of capillary height (h^2) and time (t) in the initial stage and between the capillary rise velocity (dh/dt) and reciprocal of capillary height ($1/h$) in the long-time stage were conducted and shown in Fig. 11 based on Eq. (5) and Eq. (3), respectively. As shown in Fig. 11, the linear fitting curves matched well with the experimental data, and slope k_1 and k_2 were obtained. The capillary performance parameter can be calculated from Eq. (4) and Eq. (6), respectively. The calculation results are listed in Table 2. It is found that the modified grooved wicks have higher $\Delta P_c \cdot K$ than the bare grooved wick, e.g., the S2 exhibited $\Delta P_c \cdot K$ of 3.38e-5 N in the case with gravity, which was an order of magnitude larger than that of 3.22e-6 N for the S1. However, the difference of $\Delta P_c \cdot K$ between the modified grooved

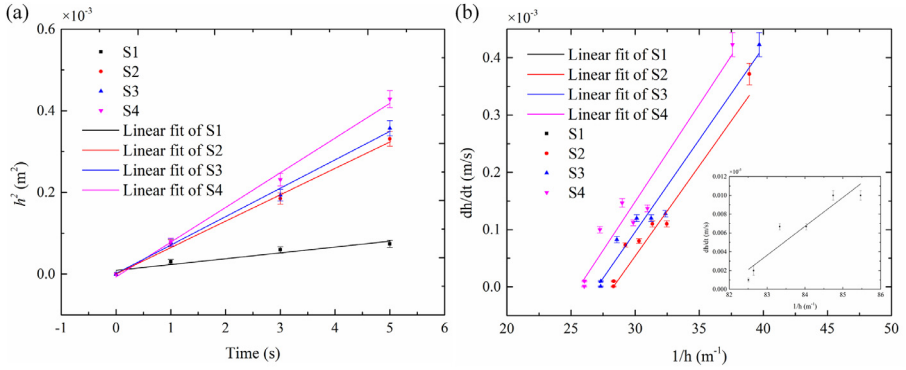

Fig. 11. Linear fits (a) between square of capillary height (h^2) and time (t) in the initial stage based on Eq. (3); (b) between capillary rise velocity (dh/dt) and reciprocal of capillary height ($1/h$) in the long-time stage based on Eq. (5).

wicks was negligible in the long-time stages. In addition, the $\Delta P_c \cdot K$ values of the modified grooved wicks in these two stages were similar. It is indicated that the influence of gravity on the capillary rise process is greatly weakened due to the capillary force of the porous microstructures, justifying the prominent comprehensive capillary performance of the modified grooved wicks. In link with the previous analysis of capillary rise height, it can be concluded that the ultrasonic modification method is an effective approach to enhance the capillary performance of the grooved aluminum wicks.

4. Conclusions

In this study, an ultrasonic modification method was developed to fabricate porous microstructures on the aluminum groove surface. Cavitation collapse impact induced by ultrasonic vibration in water was used to modify the groove surface. The behavior of the modified grooved wicks with different modification times was investigated by surface morphology characterization, wettability test and capillary rise test. Experimental results show that appropriate ultrasonic modification times can realize an excellent distribution of porous microstructures throughout the aluminum groove surface, while excessive ultrasonic modification may cause damage to the top of the grooves. After ultrasonic modification, the aluminum surface became hydrophobic and superoleophilic due to the formation of the layer of porous microstructures with a low-surface-energy organic matter coating. The negative effect of low surface energy cannot inhibit the enhancement of the capillary performance with acetone since the porous microstructures reduce the capillary radius of the wick greatly. The porous microstructures at the bottom of the groove enhanced capillary performance more significantly than that at the sidewall of the groove. The maximum capillary rise height and capillary performance parameter ($\Delta P_c \cdot K$) were increased for a factor of 3 and an order of magnitude, respectively. So, ultrasonic modification is an effective approach to enhance the capillary performance of the grooved aluminum wicks.

Declaration of Competing Interest

This manuscript has not been published or presented elsewhere in part or in entirety, and is not under consideration by another journal. All the authors have approved the manuscript and agree with submission to your esteemed journal. There are no conflicts of interest to declare.

CRediT authorship contribution statement

Guisheng Zhong: Conceptualization, Methodology, Validation, Investigation, Data curation, Formal analysis, Writing – original draft. **Yong Tang:** Investigation, Data curation, Project administration, Funding acquisition. **Xinrui Ding:** Writing – review & editing, Supervision, Project administration, Funding acquisition. **Gong Chen:** Methodology, Formal analysis, Writing – review & editing. **Zongtao Li:** Conceptualization, Validation, Formal analysis, Funding acquisition.

Acknowledgments

This work was supported by the National Natural Science Foundation of China [Grant Nos. 51735004, 51805173]; the Science and Technology Planning Project of Guangdong Province [Grant No. 2019B090910001]; the Natural Science Foundation of Guangdong Province [Grant No. 2019A1515011741]; and the Science and Technology Program of Guangzhou [Grant No. 201904010252]. One of the authors, Guisheng Zhong, would like to acknowledge financial support from the Chinese Scholarship Council (CSC No. 201906150010).

References

[1] Y. Tang, S. Hong, S. Wang, D. Deng, Experimental study on thermal performances of ultra-thin flattened heat pipes, Int. J. Heat Mass Transf. 134 (2019) 884–894.
[2] H. Tang, Y. Tang, Z. Wan, J. Li, W. Yuan, L. Lu, Y. Li, K. Tang, Review of applications and developments of ultra-thin micro heat pipes for electronic cooling, Appl. Energy 223 (2018) 383–400.
[3] F. Xin, T. Ma, Q. Wang, Thermal performance analysis of flat heat pipe with graded mini-grooves wick, Appl. Energy 228 (2018) 2129–2139.
[4] J. Supowit, T. Heflinger, M. Stubblebine, I. Catton, Designer fluid performance and inclination angle effects in a flat grooved heat pipe, Appl. Therm. Eng. 101 (2016) 770–777.
[5] Y. Li, J. He, H. He, Y. Yan, Z. Zeng, B. Li, Investigation of ultra-thin flattened heat pipes with sintered wick structure, Appl. Therm. Eng. 86 (2015) 106–118.
[6] J. Li, L. Lv, Experimental studies on a novel thin flat heat pipe heat spreader, Appl. Therm. Eng. 93 (2016) 139–146.
[7] S. Zhang, J. Chen, Y. Sun, J. Li, J. Zeng, W. Yuan, Y. Tang, Experimental study on the thermal performance of a novel ultra-thin aluminum flat heat pipe, Renew. Energy 135 (2019) 1133–1143.
[8] L. Lv, J. Li, Managing high heat flux up to 500W/cm2 through an ultra-thin flat heat pipe with superhydrophilic wick, Appl. Therm. Eng. 122 (2017) 593–600.
[9] S. Somasundaram, Y. Zhu, Z. Lu, S. Adera, H. Bin, W. Mengyao, C.S. Tan, E.N. Wang, Thermal design optimization of evaporator micropillar wicks, Int. J. Therm. Sci. 134 (2018) 179–187.
[10] D.P. McNally, R. Lewis, Y.C. Lee, Characterization of hybrid wicking structures for Flexible vapor chambers, J. Electron. Packag. Trans. ASME 141 (2019) 1–7.
[11] D. Deng, Y. Tang, G. Huang, L. Lu, D. Yuan, Characterization of capillary performance of composite wicks for two-phase heat transfer devices, Int. J. Heat Mass Transf. 56 (2013) 283–293.
[12] S.C. Wong, W.S. Liao, Visualization experiments on flat-plate heat pipes with composite mesh-groove wick at different tilt angles, Int. J. Heat Mass Transf. 123 (2018) 839–847.
[13] J. Cheng, G. Wang, Y. Zhang, P. Pi, S. Xu, Enhancement of capillary and thermal performance of grooved copper heat pipe by gradient wettability surface, Int. J. Heat Mass Transf. 107 (2017) 586–591.
[14] J. Zeng, L. Lin, Y. Tang, Y. Sun, W. Yuan, Fabrication and capillary characterization of micro-grooved wicks with reentrant cavity array, Int. J. Heat Mass Transf. 104 (2017) 918–929.

[15] J. Zeng, S. Zhang, G. Chen, L. Lin, Y. Sun, L. Chuai, W. Yuan, Experimental investigation on thermal performance of aluminum vapor chamber using micro-grooved wick with reentrant cavity array, Appl. Therm. Eng. 130 (2018) 185–194.
[16] G. Huang, W. Yuan, Y. Tang, B. Zhang, S. Zhang, L. Lu, Enhanced capillary performance in axially grooved aluminium wicks by alkaline corrosion treatment, Exp. Therm. Fluid Sci. 82 (2017) 212–221.
[17] H. Tang, Y. Tang, W. Yuan, R. Peng, L. Lu, Z. Wan, Fabrication and capillary characterization of axially micro-grooved wicks for aluminium flat-plate heat pipes, Appl. Therm. Eng. 129 (2018) 907–915.
[18] L. Lu, J. Sun, Q. Liu, X. Liu, Y. Tang, Influence of electrochemical deposition parameters on capillary performance of a rectangular grooved wick with a porous layer, Int. J. Heat Mass Transf. 109 (2017) 737–745.
[19] M. Virot, R. Pflieger, E.V. Skorb, J. Ravaux, T. Zemb, H. Möhwald, Crystalline silicon under acoustic cavitation: from mechanoluminescence to amorphization, J. Phys. Chem. C 116 (2012) 15493–15499.
[20] E.V. Skorb, D. Fix, D.G. Shchukin, H. Möhwald, D.V. Sviridov, R. Mousa, N. Wanderka, J. Schäferhans, N. Pazos-Pérez, A. Fery, D.V. Andreeva, Sonochemical formation of metal sponges, Nanoscale 3 (2011) 985–993.
[21] J. Zhang, L.X. Lian, Y. Liu, Liquid phase enhanced sintering of porous aluminum for cylindrical Al-acetone heat pipe, Int. J. Heat Mass Transf. 152 (2020) 119512.
[22] K.L. Tan, S.H. Yeo, Bubble dynamics and cavitation intensity in milli-scale channels under an ultrasonic horn, Ultrason. Sonochemistry 58 (2019) 104666.
[23] A.P. Nagalingam, S.H. Yeo, Effects of ambient pressure and fluid temperature in ultrasonic cavitation machining, Int. J. Adv. Manuf. Technol. 98 (2018) 2883–2894.
[24] F. Bai, K.A. Saalbach, L. Wang, X. Wang, J. Twiefel, Impact of time on ultrasonic cavitation peening via detection of surface plastic deformation, Ultrasonics 84 (2018) 350–355.
[25] Y. Tang, D. Deng, L. Lu, M. Pan, Q. Wang, Experimental investigation on capillary force of composite wick structure by IR thermal imaging camera, Exp. Therm. Fluid Sci. 34 (2010) 190–196.
[26] D. Deng, Y. Tang, J. Zeng, S. Yang, H. Shao, Characterization of capillary rise dynamics in parallel micro *V*-grooves, Int. J. Heat Mass Transf. 77 (2014) 311–320.
[27] B. Holley, A. Faghri, Permeability and effective pore radius measurements for heat pipe and fuel cell applications, Appl. Therm. Eng. 26 (2006) 448–462.
[28] E.W. Washburn, The dynamics of capillary flow, Phys. Rev. 17 (1921) 273–283.
[29] S.J. Kline, F.A. McClintock, Describing uncertainties in single-sample experiments, Mech. Eng. 75 (1953) 3–9.
[30] R.N. Wenzel, Resistance of solid surfaces to wetting by water, Ind. Eng. Chem. 28 (8) (1936) 988–994.
[31] E.V. Skorb, D.G. Shchukin, H. Möhwald, D.V. Andreeva, Ultrasound-driven design of metal surface nanofoams, Nanoscale 2 (5) (2010) 722–727.
[32] C.V. Ngo, D.M. Chun, Control of laser-ablated aluminum surface wettability to superhydrophobic or superhydrophilic through simple heat treatment or water boiling post-processing, Appl. Surf. Sci. 435 (2018) 974–982.
[33] S. Takeda, M. Fukawa, Y. Hayashi, K. Matsumoto, Surface OH group governing adsorption properties of metal oxide films, Thin Solid Film. 339 (1999) 220–224.
[34] J. Van den Brand, S. Van Gils, P.C.J. Beentjes, H. Terryn, J.H.W. De Wit, Ageing of aluminium oxide surfaces and their subsequent reactivity towards bonding with organic functional groups, Appl. Surf. Sci. 235 (2004) 465–474.
[35] Ö. Özkanat, B. Salgin, M. Rohwerder, J.M.C. Mol, J.H.W. de Wit, H. Terryn, Scanning Kelvin probe study of (Oxyhydr)oxide surface of aluminum alloy, J. Phys. Chem. C 116 (2012) 1805–1811.
[36] P. Larkin, Infrared and Raman Spectroscopy: Principles and Spectral Interpretation, Elsevier, 2011.
[37] A.B.D. Cassie, S. Baxter, Wettability of porous surfaces, Trans. Faraday Soc. 40 (1944) 546–551.